Inorg. Chem. **2002**, *41*, 2173–2181

Structure of the Deoxymyoglobin Model [Fe(TPP)(2-MeHIm)] Reveals Unusual Porphyrin Core Distortions

Mary K. Ellison,[†] Charles E. Schulz,*[,‡] and W. Robert Scheidt*[,†]

The Department of Chemistry and Biochemistry, University of Notre Dame, Notre Dame, Indiana 46556, and Department of Physics, Knox College, Galesburg, Illinois 61401

Received January 2, 2002

The preparation and characterization of the deoxymyoglobin model (2-methylimidazole)(tetraphenylporphinato)iron(II) is described. The preparation and crystallization from chlorobenzene leads to a new crystalline phase that has been structurally characterized. The complex is the most ordered example of a deoxymyoglobin model yet characterized. The X-ray structure determination reveals a number of distortions both in the iron coordination group and in the porphyrin core that result from the steric bulk of the axial ligand. Some of these distortions have been noted previously in related species; however, the demonstration of porphyrin core distortions and an asymmetry in the Fe–N_p bond distances are new observations. These may have functional significance for this important type of heme protein coordination group. The new structure emphasizes that high-spin iron(II) porphyrinate derivatives display substantial structural pliability with significant variations in iron atom displacements, porphyrin core hole size, and axial and equatorial Fe–N bond lengths. The new complex has also been characterized by zero-field and applied field magnetic Mössbauer spectroscopy. Mössbauer parameters are characteristic for high-spin iron, although they also reveal an extremely rhombic site for iron(II). Crystal data at 130 K for [Fe(TPP)(2-MeHIm)]·1.5C_6H_5Cl: $a = 12.334(3)$ Å, $b = 13.515(6)$ Å, $c = 14.241(7)$ Å, $\alpha = 70.62(3)°$, $\beta = 88.29(2)°$, $\gamma = 88.24(3)°$, triclinic, space group, $P\bar{1}$, $V = 2238(2)$ Å^3, $Z = 2$.

Introduction

An exceedingly important coordination group for heme proteins is the five-coordinate heme group with an axial histidine as the fifth ligand, often called the proximal histidine in the proteins. Protein derivatives with both 2+ and 3+ oxidation states of iron are represented. Common functions for such five-coordinate histidine-ligated heme proteins are those of sensors and carriers of small molecules, particularly the diatomic species NO, CO, and O_2. The five-coordinate species are high-spin complexes; the binding of the diatomic molecule leads to six coordination, a change in spin state, and a significant change in structure around the iron atom. The most celebrated example of the transition between five coordination and six coordination is the stereochemical features fundamental in the cooperativity mechanism for oxygen binding by hemoglobins.[1−3] Features of possible significance in hemoglobin cooperativity include the movement of the iron atom with respect to the porphyrin plane, changes in axial bond length, changes in porphyrin core conformation, and changes in orientation and off-axis tilts of the proximal histidine.[4,5]

Despite the importance of five-coordination in heme proteins, simple porphyrin analogues have not been intensively studied. The preparation of simple iron porphyrinates containing a single axial imidazole ligand is difficult because the binding constant of the second imidazole is larger than the binding constant of the first imidazole owing to the accompanying spin-state transition from high spin to low spin. Thus, the synthesis of six-coordinate bis-ligated complexes is much easier than that of five-coordinate species. A synthetic strategy for preparing five-coordinate imidazole-ligated high-spin iron(II) derivatives was reported by Reed

* To whom correspondence should be addressed. E-mail: W.R.Scheidt.1@nd.edu (W.R.S.).
[†] University of Notre Dame.
[‡] Knox College.

(1) Perutz, M. F. *Nature* **1970**, *228*, 226.
(2) Perutz, M. F. *Nature* **1972**, *237*, 495.
(3) Perutz, M. F.; Fermi, G.; Luisi, B.; Shaanan, B.; Liddington, R. C. *Acc. Chem. Res.* **1987**, *20*, 309.
(4) Paoli, M.; Dodson, G.; Liddington, R. C.; Wilkinson, A. J. *J. Mol. Biol.* **1997**, *271*, 161.
(5) Baldwin, J. M.; Chothia, C. *J. Mol. Biol.* **1979**, *129*, 175.

10.1021/ic020012g CCC: $22.00
Published on Web 03/23/2002

and Collman in 1973[6] and used the sterically hindered 2-methylimidazole ligand. It was expected that this ligand would lead to a significantly distorted molecule only if six-coordinate species were formed. However, stereochemical issues concerning five-coordinate species remain. The crystalline complex of [Fe(TPP)(2-MeHIm)][7] prepared by Reed and Collman was structurally characterized in the laboratory of the late Prof. J. L. Hoard. A preliminary report of the structure was given at an ACS meeting,[8] and results were additionally cited and used by Hoard and Scheidt,[9] but complete structural details were never published. One crystallographic feature that marred the metrical usefulness of the structure was the presence of crystallographically required 2-fold disorder normal to the porphyrin plane. This 2-fold axis leads to positional disorder in the axial imidazole and significantly limits the accuracy of some features involving the axial ligand and possibly that of the porphyrin ligand as well. A related species, [Fe(TpivPP)(2-MeHIm)], also displayed this type of disorder[10] and suffers the same limitations. As described below, we report the structure of a new, more ordered variant of the five-coordinate species [Fe(TPP)(2-MeHIm)] that reveals a number of stereochemically important features for iron(II) porphyrinates that are possibly functionally significant.

The preparation of [Fe(TPP)(2-MeHIm)] is an outgrowth of an attempt to obtain a definitive resonance Raman study of the only spin-state/coordination number combination still wanting.[11,12] The missing combination is that of the (probably rare) six-coordinate high-spin iron(II) derivative. Since resonance Raman spectroscopy has proven to be invaluable in the assignment of spin-state/coordination number combinations in a variety of hemoprotein derivatives, we thought this issue deserved to be re-explored. The choice of a molecule for Raman study was the species $[Fe(TPP)(THF)_2]$, which was structurally characterized in 1980[13] and was the further subject of an experimental electron density study in 1986.[14] Crystalline $[Fe(TPP)(THF)_2]$ was resynthesized for study by Raman spectroscopy. As part of this investigation of $[Fe(TPP)(THF)_2]$, we also prepared crystalline, five-coordinate, high-spin [Fe(TPP)(2-MeHIm)] for parallel study by Raman spectroscopy.

The crystalline [Fe(TPP)(2-MeHIm)] species that we prepared was found to crystallize in a new crystal system, different from that of the earlier study of [Fe(TPP)(2-MeHIm)].[8] Most importantly, this new crystalline system does not demand any disorder associated with the axial or porphyrin ligand. Accordingly, we carried out a structure determination of this new crystalline form of [Fe(TPP)(2-MeHIm)]. Although we found a small disorder problem involving the axial ligand, we have obtained a structure that does not have structural features obscured by 2-fold disorder of the axial ligand. Most interestingly, the steric bulk of the 2-methylimidazole ligand leads not only to to an asymmetrical orientation of the axial ligand, which had been previously noted, but also to effects on the porphyrin ligand conformation as well. The sterically demanded tilting of the axial ligand in binding to iron, which leads to an orientation of the $Fe-N_{Im}$ that is 8.3° from the heme normal, is apparently transmitted into an asymmetric interaction between iron and the porphyrin ligand. This is manifested in an asd asymmetrically distorted nonplanar porphyrin core and in apparent nonequivalent *equatorial* $Fe-N_p$ bond distances.

Experimental Section

General Information. Chlorobenzene was washed with concentrated sulfuric acid and then with water until the aqueous layer was neutral, dried with $MgSO_4$, and distilled twice over P_2O_5 under argon. Benzene and hexanes were distilled over sodium benzophenone. Ethanethiol (Aldrich) was used as received. 2-Methylimidazole (Aldrich) was recrystallized from toluene/methanol and dried under vacuum. All other chemicals were used as received from Aldrich or Fisher. *meso*-Tetraphenylporphyrin (H_2TPP) was prepared according to Adler et al.[15] [Fe(TPP)Cl] was prepared according to a modified Adler preparation;[16] $[Fe(TPP)]_2O$ was prepared from [Fe(TPP)Cl].[17] Mössbauer measurements were performed on a constant acceleration spectrometer at 4.2−293 K in zero field and at 4.2 K in 6 and 9 T fields using a superconducting magnet system (Knox College). The solid-state Mössbauer sample was immobilized in Apiezon grease.

Synthesis of [Fe(TPP)(2-MeHIm)]·1.5C$_6$H$_5$Cl. The following reactions were done using standard Schlenk techniques. [Fe(II)(TPP)] was prepared by reduction of $[Fe(TPP)]_2O$ (65 mg, 0.04 mmol) with ethanethiol (∼ 1 mL) in ∼ 15 mL benzene according to Stolzenberg et al.[18] The benzene solution was stirred overnight followed by solvent removal under vacuum. The solid [Fe(II)(TPP)] was never exposed to air to avoid the easily formed $[Fe(TPP)]_2O$. Excess 2-methylimidazole (32 mg, 0.40 mmol) in 15 mL of dry

(6) Collman, J. P.; Reed, C. A. *J. Am. Chem. Soc.* **1973**, *95*, 2048.
(7) Abbreviations: OEP, dianion of 2,3,7,8,12,13,17,18-octaethylporphyrin; Piv_2C_8P, dianion of α,α,5,15-[2,2′-(octanediamido)diphenyl]-α,α,-10,20-bis(*o*-pivalamidophenyl)porphyrin; TMP, dianion of 5,10,15,20-tetramesitylporphyrin; TPP, dianion of 5,10,15,20-tetraphenylporphyrin; TpivPP, dianion of α,α,α,α-tetrakis(*o*-pivalamidophenyl)porphyrin or picket fence porphyrin; THF, tetrahydrofuran; 1-MeIm, 1-methylimidazole; 1,2-Me_2Im, 1,2-dimethylimidazole; 2-MeHIm, 2-methylimidazole; 2-$MeIm^-$, 2-methylimidazolate.
(8) (a) Collman, J. P.; Kim, N.; Hoard, J. L.; Lang, G.; Radonovich, L. J.; Reed, C. A. *Abstracts of Papers*; 167th National Meeting of the American Chemical Society; Los Angeles, CA, April 1974; American Chemical Society: Washington, DC; INOR 29. (b) Hoard, J. L., personal communication to W.R.S. In particular, Prof. Hoard provided a complete set of atomic coordinates for the molecule.
(9) Hoard, J. L.; Scheidt, W. R. *Proc. Natl. Acad. Sci. U.S.A.* **1973**, *70*, 3919.
(10) Jameson, G. B.; Molinaro, F. S.; Ibers, J. A.; Collman, J. P.; Brauman, J. I.; Rose, E.; Suslick, K. S. *J. Am. Chem. Soc.* **1980**, *102*, 3224.
(11) Mylrajan, M.; Andersson, L. A.; Sun, J.; Loehr, T. M.; Thomas, C. S.; Sullivan, E. P., Jr.; Thomson, M. A.; Long, K. M.; Anderson, O. P.; Strauss, S. H. *Inorg. Chem.* **1995**, *34*, 3953.
(12) Kincaid, J. R. In *The Porphyrin Handbook*; Kadish, K. M.; Smith, K. M.; Guilard, R.; Academic Press: San Diego, CA, 2001; Chapter 51.
(13) Reed, C. A.; Mashiko, T.; Scheidt, W. R.; Spartalian, K.; Lang, G. *J. Am. Chem. Soc.* **1980**, *102*, 2302.
(14) Lecomte, C.; Blessing, R. H.; Coppens, P.; Tabard, A. *J. Am. Chem. Soc.* **1986**, *108*, 6942.
(15) Adler, A. D.; Longo, F. R.; Finarelli, J. D.; Goldmacher, J.; Assour, J.; Korsakoff, L. *J. Org. Chem.* **1967**, *32*, 476.
(16) (a) Adler, A. D.; Longo, F. R.; Kampus, F.; Kim, J. *J. Inorg. Nucl. Chem.* **1970**, *32*, 2443. (b) Buchler, J. W. In *Porphyrins and Metalloporphyrins*; Smith, K. M., Ed.; Elsevier Scientific Publishing: Amsterdam, The Netherlands, 1975; Chapter 5.
(17) (a) Fleischer, E. B.; Srivastava, T. S. *J. Am. Chem. Soc.* **1969**, *91*, 2403. (b) Hoffman, A. B.; Collins, D. M.; Day, V. W.; Fleischer, E. B.; Srivastava, T. S.; Hoard, J. L.; *J. Am. Chem. Soc.* **1972**, *94*, 3620.
(18) Stolzenberg, A. M.; Strauss, S. H.; Holm, R. H. *J. Am. Chem. Soc.* **1981**, *103*, 4763.

degassed chlorobenzene was added by cannula to the solid [Fe(II)(TPP)] and stirred for 15 min. X-ray quality crystals were obtained in sealed 8 mm diameter glass tubes by liquid diffusion using hexanes as the nonsolvent.

X-ray Structure Determination. The structure determination was carried out on a Nonius FAST area-detector diffractometer with a Mo rotating anode source ($\bar{\lambda} = 0.71073$ Å). Our detailed methods and procedures for small molecule X-ray data collection with the FAST system have been described previously.[19] Data collection was performed at 130(2) K. A dark purple crystal of [Fe(TPP)(2-MeHIm)]·1.5C_6H_5Cl with dimensions 0.63 × 0.33 × 0.17 mm^3 was used for the structure determination. The structure was solved using the direct methods program SHELXS-86;[20] subsequent difference Fourier syntheses led to the location of most of the remaining non-hydrogen atoms. The 2-methylimidazole was found to be disordered over two positions: a major and a minor orientation. A rigid body model using a previously structurally characterized 2-methylimidazole[21] for the six atoms of each group was applied. The constraints for the major imidazole ligand were released near the end of the refinement. The thermal displacement parameters for N(5) and N(5B) as well as N(6) and N(6B) were constrained to be equivalent. The final refinement of the group occupancy coefficients converged to 0.854(4) and 0.146. One of the chlorobenzene solvent molecules was found to be disordered over two positions related by an inversion center. The molecule was given a total group occupancy coefficient of 0.50 and was refined as a rigid group to help locate "missing" atoms.

The structure was refined against F^2 with the program SHELXL-93[22] in which all data collected were used including negative intensities. All non-hydrogen atoms, except those of the minor 2-methylimidazole component and the nitrogen atoms of the major 2-methylimidazole component, were refined anisotropically. Hydrogen atoms of the porphyrin ligands and the solvent molecules were idealized with the standard SHELXL-93 idealization methods. The hydrogen atoms of the major 2-methylimidazole component were located directly from a difference Fourier and subsequently idealized while allowing the torsion angles to refine. A modified[24] version of the absorption correction program DIFABS was applied. Brief crystal data for [Fe(TPP)(2-MeHIm)]·1.5C_6H_5Cl are listed in Table 1. Complete crystallographic details, atomic coordinates, anisotropic thermal parameters, and fixed hydrogen atom coordinates are included in the Supporting Information (Tables S1, S2 and S5, S6).

Results

An ORTEP-III diagram of the [Fe(TPP)(2-MeHIm)] molecule is given in Figure 1.[26] The labeling scheme is consistent with all other ORTEP diagrams and the tables. Only the major (85%) orientation of the imidazole ligand is displayed. Supporting Information Figure S1 gives the same view as Figure 1 except that it shows both orientations of the axial imidazole ligand; the minor orientation is given in boundary ellipsoid format. The two imidazole planes are essentially coplanar; the dihedral angle between the two imidazole planes is 1.5°. The dihedral angle between the plane defined by N(1), Fe, and N(5) and the plane of the major imidazole is 24°. The dihedral angle between the plane of the imidazole ligand and the 24-atom mean porphyrin plane is 89.3°.

Figure 2 is a formal diagram displaying the displacements of each atom of the porphyrin core from the mean plane of the four pyrrole nitrogen atoms. The orientation of the 2-MeHIm ligand including the dihedral angle is also shown; the circle represents the position of the methyl group. Values of the four individual Fe−N_p bond distances are also given on the diagram. Values of the displacements of the porphyrin core atoms from the mean plane of the 24-atom core are

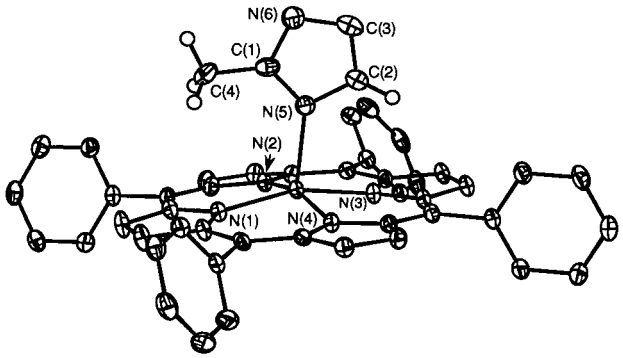

Figure 1. ORTEP diagram of [Fe(TPP)(2-MeHIm)]. Solvent molecules and most of the hydrogen atoms are omitted for clarity. Major orientation of the imidazole ligand is shown. Thermal ellipsoids are drawn at the 50% probability level.

Table 1. Crystallographic Details for [Fe(TPP)(2-MeHIm)]·1.5C_6H_5Cl

formula	$C_{48}H_{34}FeN_6$·1.5C_6H_5Cl
FW, amu	919.49
a, Å	12.334(3)
b, Å	13.515(6)
c, Å	14.241(7)
α, deg	70.62(3)
β, deg	88.29(2)
γ, deg	88.24(3)
V, Å^3	2237.7(16)
space group	$P\bar{1}$
Z	2
D_{calcd}, g/cm^3	1.365
F(000)	954
μ, mm^{-1}	0.474
cryst dimens, mm^3	0.63 × 0.33 × 0.17
absorption correction	DIFABS
λ, Å	0.71073
T, K	130(2)
total data collected	19827
unique data	10958 (R_{int} = 0.058)
unique obsd data [$I > 2\sigma(I)$]	8588
refinement method	on F^2 (SHELXL-93)
final *R* indices [$I > 2\sigma(I)$]	R1 = 0.0564, wR2 = 0.1346
final *R* indices [for all data]	R1 = 0.0778, wR2 = 0.1504

(19) Scheidt, W. R.; Turowska-Tyrk, I. *Inorg. Chem.* **1994**, *33*, 1314.
(20) Sheldrick, G. M. *Acta Crystallogr.* **1990**, *A46*, 467.
(21) Scheidt, W. R.; Geiger, D. K.; Lee, Y. J.; Reed, C. A.; Lang, G. *J. Am. Chem. Soc.* **1985**, *107*, 5693.
(22) Sheldrick, G. M. *J. Appl. Crystallogr.*, in preparation.
(23) R1 = $\sum||F_o| - |F_c||/\sum|F_o|$ and wR2 = $\{\sum[w(F_o^2 - F_c^2)^2]/\sum[wF_o^4]\}^{1/2}$. The conventional *R* factors R1 are based on *F*, with *F* set to zero for negative F^2. The criterion of $F^2 > 2\sigma(F^2)$ was used only for calculating R1. *R* factors based on F^2 (wR2) are statistically about twice as large as those based on *F*, and *R* factors based on *all* data will be even larger.
(24) The process is based on an adaptation of the DIFABS[25] logic to area detector geometry by Karaulov: Karaulov, A. I. School of Chemistry and Applied Chemistry, University of Wales, College of Cardiff, Cardiff CF1 3TB, U.K. Personal communication.
(25) Walker, N. P.; Stuart, D. *Acta Crystallogr., Sect. A* **1983**, *A39*, 158.
(26) Burnett, M. N.; Johnson, C. K. *ORTEP-III*; Report ORNL-6895; Oak Ridge National Laboratory: Oak Ridge, TN, 1996.

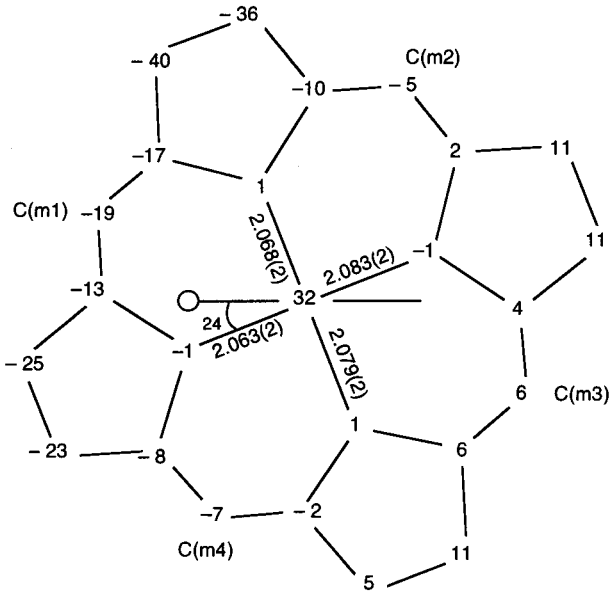

Figure 2. Formal diagram of the porphyrinato core of [Fe(TPP)(2-MeHIm)]. Shown are the perpendicular displacements, in units of 0.01 Å, from the 4-nitrogen atom mean plane of the porphyrin core. Values of the four equatorial Fe−N_p bond distances are given. Orientation of the 2-MeHIm ligand including the dihedral angle is shown; the methyl group is represented by the circle.

given in Figure S2 of the Supporting Information. Complete listings of the bond lengths and angles are included in the Supporting Information (Tables S3 and S4). Table 2 lists selected bond lengths and angles for [Fe(TPP)(2-MeHIm)] and other imidazole and/or five-coordinate iron derivatives for subsequent discussion. To distinguish between the two structure determinations of [Fe(TPP)(2-MeHIm)], we have appended the suffix -(2-fold) to the formula of the early structure[8] to denote its required crystallographic symmetry and no suffix to the present structure because there is no required symmetry.

Figure 3 displays the Mössbauer spectra obtained for [Fe(TPP)(2-MeHIm)] in zero field and 6 and 9 T applied fields. The Mössbauer spectra for [Fe(TPP)(2-MeHIm)] in zero field were fit assuming Lorentzian line shapes. The values of the quadrupole splitting and isomer shift obtained were −2.43 and 0.94 mm/s, respectively, with the sign of the quadrupole splitting obtained from an analysis of the spectra obtained in applied magnetic field.

Discussion

Mössbauer Studies. The zero-field values of the quadrupole splitting and isomer shift for the current form of [Fe(TPP)(2-MeHIm)] are typical for high-spin iron(II) porphyrinates.[36] The isomer shift and quadrupole splitting values are similar to those reported earlier by Kent et al.[37] for polycrystalline samples of [Fe(TPP)(2-MeHIm)] and [Fe(TPP)(1,2-Me_2Im)]. Values for two forms of [Fe(TPP)(2-MeHIm)] and [Fe(TPP)(1,2-Me_2Im)], as well as those for deoxymyoglobin and deoxyhemoglobin, are listed in Table 3. The asymmetry parameter (η) is large in all species and equal within the experimental uncertainties. The slightly different values of the quadrupole splitting for the two forms of [Fe(TPP)(2-MeHIm)] are consistent with the expectation that the presently described preparation and the earlier preparation do indeed result in distinctly different crystalline phases. Interestingly, an even bigger difference between the two crystalline forms is the appearance of the high-field spectra at 4.2 K. The spectrum previously reported[37] has well-resolved features (e.g., six lines) at 6 T while our form has a broad, rather featureless spectrum at both 6 and 9 T (Figure 3). The rather featureless spectra are similar to those found for [Fe(TPP)(1,2-Me_2Im)], deoxymyoglobin, and deoxyhemoglobin.[40] These broad spectra led Kent et al.[37] to model the spectra using an ω tensor fit. The ω tensor fits are a useful prelude to developing a spin Hamiltonian model. Kent et al. used a spin Hamiltonian model for modeling the applied-field spectra of [Fe(TPP)(2-MeHIm)], as did we. For the other, related compounds, they only used ω tensor fits. There are some significant differences between the two sets of resulting fit parameters for the two crystalline forms of [Fe(TPP)(2-MeHIm)], which are discussed later.

The Mössbauer data shown in Figure 3 were fit using the spin Hamiltonian model used by Kent et al.:[37]

$$H = D[S_z^2 - 1/3S(S+1)] + E(S_x^2 - S_y^2) + \vec{H}\cdot\tilde{g}\cdot\vec{S} + H^Q - g_N^*\beta_N\vec{H}\cdot\vec{I} + \vec{S}\cdot\tilde{A}^*\cdot\vec{I}$$

where D and E are the axial and rhombic zero-field splitting parameters that describe the fine structure of the S

(27) Momenteau, M.; Scheidt, W. R.; Eigenbrot, C. W.; Reed, C. A. *J. Am. Chem. Soc.* **1988**, *110*, 1207.
(28) Mandon, D.; Ott-Woelfel, F.; Fischer, J.; Weiss, R.; Bill, E.; Trautwein, A. X. *Inorg. Chem.* **1990**, *29*, 2442.
(29) Schappacher, M.; Ricard, L.; Weiss, R.; Montiel-Montoya, R.; Gonser, U.; Bill, E.; Trautwein, A. X. *Inorg. Chim. Acta* **1983**, *78*, L9.
(30) Caron, C.; Mitschler, A.; Riviere, G.; Schappacher, M.; Weiss, R. *J. Am. Chem. Soc.* **1979**, *101*, 7401.
(31) Nasri, H.; Fischer, J.; Weiss, R.; Bill, E.; Trautwein, A. X. *J. Am. Chem. Soc.* **1987**, *109*, 2549.
(32) Steffen, W. L.; Chun, H. K.; Hoard, J. L.; Reed, C. A. *Abstracts of Papers*, 175th National Meeting of the American Chemical Society, Anaheim, CA, March 1978; American Chemical Society: Washington, DC, 1978; INOR 15. (b) Hoard, J. L. Personal communication.
(33) Geiger, D. K.; Lee, Y. J.; Scheidt, W. R. *J. Am. Chem. Soc.* **1984**, *106*, 6339.
(34) Scheidt, W. R.; Kirner, J. F.; Hoard, J. L.; Reed, C. A. *J. Am. Chem. Soc.* **1987**, *109*, 1963.
(35) Munro, O. Q.; Serth-Guzzo, J. A.; Turowska-Tyrk, I.; Mohanrao, K.; Shokhireva, T. Kh.; Walker, F. A.; Debrunner, P. G.; Scheidt, W. R. *J. Am. Chem. Soc.* **1999**, *121*, 11144.
(36) Debrunner, P. G. In *Iron Porphyrins Part 3*; Lever, A. B. P.; Gray, H. B., Eds.; VCH Publishers Inc.: New York, 1983; Chapter 2.
(37) Kent, T. A.; Spartalian, K.; Lang, G.; Yonetani, T.; Reed, C. A.; Collman, J. P. *Biochim. Biophys. Acta* **1979**, *580*, 245.
(38) Kent, T. A.; Spartalian, K.; Lang, G.; Yonetani, T. *Biochim. Biophys. Acta* **1977**, *490*, 331.
(39) Kent, T. A.; Spartalian, K.; Lang, G. *J. Chem. Phys.* **1979**, *71*, 4899.
(40) Early papers on deoxymyoglobin by Trautwein and Eicher[41,42] argued, on the basis of both experimental results and electronic structure calculations, for axial symmetry ($\eta = 0$) of the electric field gradient (EFG), with positive V_{zz} and one of the EFG's principal axes along the heme normal. Zimmermann[43] and Maeda et al.[44] later showed that the EFG components were not uniquely determined by the data of Trautwein and Eicher; a manifold of values of the EFG fit the data equally well. Kent et al.[38] analyzed high-field, variable-temperature Mössbauer spectra to conclude the EFG was indeed nonaxial (η = 0.7) and that V_{zz} was negative. Furthermore, their results implied that the EFG did not have a principal axis near the heme normal; V_{zz} was rotated by 58° (or 122°) from the normal.

Table 2. Selected Bond Distances (Å) and Angles (deg) for [Fe(Porph)(Im)][a]

complex[b]	Fe−N_p[c,d]	Fe−N_{im}[d]	ΔN_4[d,e]	Δ[d,f]	Ct···N[d]	Fe−N−C[g,h]	Fe−N−C[g,i]	θ[g,j]	ϕ[g,k]	ref
				Iron(II)						
[Fe(TPP)(2-MeHIm)](2-fold)	2.086(8)	2.161(5)	0.42	0.55	2.044	131.4(4)	122.6(4)	10.3	6.5	8
[Fe(TpivPP)(2-MeHIm)]	2.072(6)	2.095(6)	0.40	0.43	2.033	132.1(8)	126.3(7)	9.6	22.8	10
[Fe(Piv_2C_8P)(1-MeIm)]	2.07(2)	2.13(2)	0.31	0.34	2.051	126.5	120.4	5.0	34.1	27
[Fe(TPP)(2-MeHIm)]·1.5C_6H_5Cl	2.073(9)	2.127(3)[l]	0.32	0.38	2.049	131.1(2)	122.9(2)	8.3	24.0	this work
[Fe(TpivPP)(2-$MeIm^-$)]$^-$	2.11(2)	2.002(15)	0.52	0.65	2.045	NR[m]	NR	5.1	14.7	28
[Fe(TpivPP)Cl]$^-$	2.108(15)	2.301(2)[n]	0.53	0.59	2.040					29
[Fe(TpivPP)(SC_6HF_4)]$^-$	2.076(20)	2.370(3)[o]	0.42	NR	2.033					29
[Fe(TPP)(SC_2H_5)]$^-$	2.096(4)	2.360(2)[o]	0.52	0.62	2.030					30
[Fe(TpivPP)(O_2CCH_3)]$^-$	2.107(2)	2.034(3)[p]	0.55	0.64	2.033					31
[Fe(TpivPP)(OC_6H_5)]$^-$	2.114(2)	1.937(4)[p]	0.56	0.62	2.037					31
[Fe(TPP)(1-MeIm)$_2$][q]	1.997(4)	2.014(5)	0.0[r]	0.0r	1.997	128.2	128.3	1.1	14.7	32
[Fe(TPP)(THF)$_2$]	2.057(4)	2.351(3)[s]	0.0[r]	0.0[r]	2.057					13
				Iron(III)						
[Fe(OEP)(2-MeHIm)]$^+$	2.038(6)	2.068(4)	0.35	0.36	2.008	131.7(3)	122.1(3)	5.0	3.9	21
[Fe(OEP)(2-MeHIm)$_2$]$^+$	2.041(11)	2.275(1)	0.0[r]	0.0[r]	2.041	134.15(10)	120.76(9)	3.2	22.2	33
[Fe(TPP)((2-MeHIm)$_2$]$^{+q}$	1.970(4)	2.012(4)	0.0	0.0	1.970	132.8	120.6	~4, 4	33, 32	34
[Fe(TMP)((1,2-Me_2Im)$_2$]$^{+q}$	1.937(12)	2.004(5)	0.01	0.01	1.937	134.6	119.8	NR	45, 45	35
[Fe(OEP)(1-MeIm)$_2$]$^{+q}$	2.004(2)	1.975(2)	0.0[r]	0.0[r]	2.004	NR	NR	NR	20	11

[a] Estimated standard deviations are given in parentheses. [b] Unless noted otherwise, complex is high spin. [c] Averaged value. [d] In Å. [e] Displacement of iron from the mean plane of the four pyrrole nitrogen atoms. [f] Displacement of iron from the 24-atom mean plane of the porphyrin core. [g] Value in degrees. [h] 2-Carbon, sometimes methyl substituted. [i] Imidazole 4-carbon. [j] Off-axis tilt (deg) of the Fe−N_{Im} bond from the normal to the porphyrin plane. [k] Dihedral angle between the plane defined by the closest N_p−Fe−N_{im} and the imidazole plane in deg. [l] Major imidazole orientation. [m] Not reported. [n] Chloride. [o] Thiolate. [p] Anionic oxygen donor. [q] Low spin. [r] Six-coordinate; required to be zero by symmetry. [s] Neutral oxygen donor.

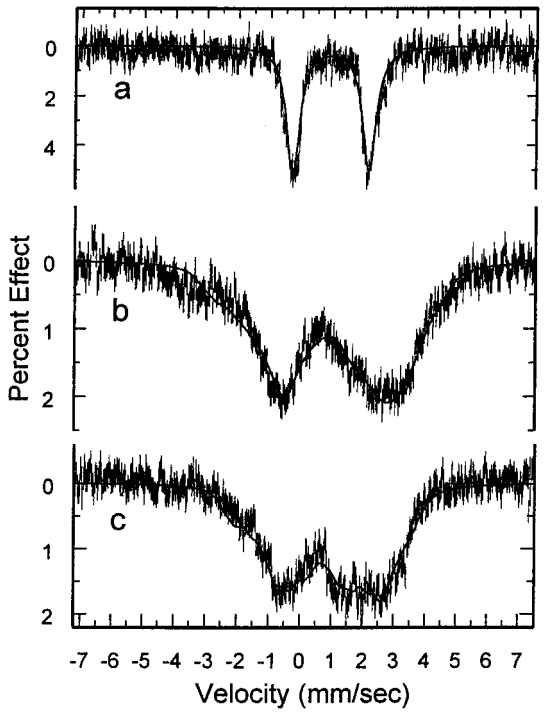

Figure 3. Mössbauer spectra obtained for [Fe(TPP)(2-MeHIm)] in (a) zero magnetic field and in applied magnetic fields of (b) 6 T and (c) 9 T. Solid lines give the fits to the data using the model parameters described in the text. All measurements illustrated were done at 4.2 K.

$= 2$ multiplet, $\tilde{A}^*$ is the magnetic hyperfine tensor, and H^Q gives the nuclear quadrupole interaction

$$H^Q = \frac{eQV_{zz}}{12}[3I_z^2 - I(I+1) + \eta(I_x^2 - I_y^2)]$$

Q is the quadrupole moment of the ^{57}Fe nucleus, and $\eta = (V_{xx} - V_{yy})/V_{zz}$, where V_{ii} are components of the electric field gradient. The quadrupole splitting and isomer shift were constrained to the values determined from the zero-field data

Table 3. Mössbauer Parameters for Five-Coordinate, High-Spin Imidazole-Ligated Iron(II) Porphyrinates

complex	ΔE_Q, mm/s	δ, mm/s	η	ref
[Fe(TPP)(2-MeHIm)]	−2.43	0.94	0.9	this work
[Fe(TPP)(2-MeHIm)](2-fold)	−2.28	0.93	0.8	37
[Fe(TPP)(1,2-Me_2Im)]	−2.16	0.92	0.7	37
deoxymyoglobin	−2.22	0.92	0.7	37, 38
deoxyhemoglobin	−2.40	0.92	0.7	37

(spectrum a, Figure 3). The signs of V_{zz} and D were taken to be negative, consistent with earlier results. We also assume that the slow spin fluctuation limit applies at 4.2 K in calculating simulated spectra. Simultaneous fits to spectra b and c were obtained by least squares minimization using a downhill simplex method.[45]

To obtain the best simultaneous fits to the applied-field spectra at 6 and 9 T, we had to allow a nonaxial magnetic hyperfine tensor ($A^*_{xx} \neq A^*_{yy}$) and also allow the principal axes of the quadrupole tensor to rotate with respect to the axes of the g and $\tilde{A}^*$ tensors. The parameters that were varied for the simultaneous fits were D, E, the components of $\tilde{A}^*$, η, and the Euler angles relating the principal axes of the quadrupole and D tensors. The final parameters of the fit are given in Table 4. As discussed later, there are some significant difference in this fit and the one reported previously by Kent et al.[37]

In their analysis of Mössbauer spectra of [Fe(TPP)(2-MeHIm)](2-fold), Kent et al.[37] reported parameter values for 4.2 K spectra, which we give in Table 4. The first set of these parameters are a compromise to give simultaneous fits

(41) Eicher, H.; Trautwein, A. X. *J. Chem. Phys.* **1969**, *50*, 2540.
(42) Eicher, H.; Trautwein, A. X. *J. Chem. Phys.* **1970**, *52*, 932.
(43) Zimmermann, R. *Nucl. Instrum. Methods* **1975**, *128*, 537.
(44) Maeda, Y.; Harami, T.; Trautwein, A. X.; Gonser, U. *Z. Naturforsch.* **1976**, *31b*, 487.
(45) Press, W. H.; Teukolsky, S. A.; Vetterling, W. T.; Flannery, B. P., *Numerical Recipes in C, The Art of Scientific Computing*, 2nd ed.; Cambridge University Press: New York, 1992; p 408.

Table 4. Mössbauer Parameters for the Two Crystalline Forms of [Fe(TPP)(2-MeHIm)]

complex	D, cm^{-1}	E/D	$A^*_{xx}/g^*_{xx}\beta_N$, T	$A^*_{yy}/g^*_{xx}\beta_N$, T	$A^*_{zz}/g^*_{xx}\beta_N$, T	α^a	β^a	γ^a	ref
[Fe(TPP)(2-MeHIm)]	−4.4	0.33	−13.6	−19.8	−2.5	12	56	0	this work
[Fe(TPP)(2-MeHIm)](2-fold)	−5.0	0.34	−5.1	−5.1	−9.6				37
	−5.4	0.51	−6.6	−6.6	−10.4				37
	−2.9	1.0	−11.3	−11.3	−5.4	0	90	0	this work
deoxyMb	4.8	0.0	−4.9	−4.7	−10.9				38,39

[a] Euler angles for rotation of the electric field gradient with respect to the g tensor. See Tinkham, M. Group *Theory and Quantum Mechanics*; McGraw-Hill Book Company: New York, 1964; p 102.

to spectra taken at 6T and at lower fields, while the second line gives the optimum fit for the 6T spectra alone. The third line is an alternate fit we have calculated (vide infra).

These parameters, and the spectra they fit, match reasonably closely the spectra and parameters of deoxymyoglobin, Table 4.[38,39] While it might then be tempting to conclude that the near-axial $\tilde{A}^*$ tensors in these fits indicate axial symmetry at the iron site in the molecules, that conclusion would be ill-founded. This is made clear by the large rhombicity E/D in the zero-field splitting, as well as the large values for the asymmetry parameter (η) of the EFG.

Important conclusions Kent et al. make are (i) the sixth d-electron is in an orbital of predominantly prolate symmetry (i.e., d_{z^2}) and the z-axis of the zero-field splitting is nearly orthogonal to that of the electric field gradient, (ii) the splitting of the ground sextet is small, with $|D| \sim 5$ cm^{-1}, and the lowest pair of states in the $S = 2$ multiplet is separated by no more than 1.5 cm^{-1}, and (iii) the $\tilde{A}^*$ tensor as a whole is unexpectedly small when compared with a crystal field theory calculation and has A^*_{zz} as its largest component. The validity of this last conclusion hangs on the assumption that the EFG tensor is aligned with the $\tilde{A}^*$ tensor. However, if the z-axis (largest component) of the EFG is rotated to lie near the heme plane, an $\tilde{A}^*$ tensor of nearly axial symmetry with A^*_{zz} smallest can be found which fits the spectra equally well. In light of the varying parameters, which fit the spectra equally well, caution is required in reaching physical conclusions.

The Mössbauer parameters for our crystalline form of [Fe(TPP)(2-MeHIm)] share with deoxymyoglobin the large negative quadrupole splitting and a small highly rhombic zero-field splitting tensor (D and E/D). Values for these parameters were found through simultaneous fits of Mössbauer spectra at 6 and 9 T. As shown in Table 3, the sign and rhombicity of the EFG and zero-field splitting parameters are in general agreement with those of deoxymyoglobin and [Fe(TPP)(2-MeHIm)](2-fold). Thus, we can conclude that the nature of the ground $S = 2$ multiplet for our compound is not too dissimilar from the others. However, acceptable fits to both the 6 and 9 T spectra for our crystalline form of [Fe(TPP)(2-MeHIm)] were found only when the z axis of the EFG tensor was rotated through $\beta = 56°$ in the xz plane of the $\tilde{A}^*$ and g tensors (Table 4).[46] Crystal field theory calculations on several high-spin ferrous systems have demonstrated that it is not unusual for the symmetry to be sufficiently low that the EFG, $\tilde{A}^*$, and g tensor axes are not aligned.[39,47,48] Such a complete crystal field calculation is beyond the scope of this paper. But a reasonable conclusion is that the Mössbauer data are telling us this crystalline form of [Fe(TPP)(2-MeHIm)] is of greatly reduced symmetry relative to the other compounds. Both the observed rotation of the EFG tensor and the difference between A^*_{xx} and A^*_{yy} lead us to this conclusion.

Furthermore, this low symmetry is reflected in the unusual features of the molecular structure for this compound that are described subsequently. The current results suggest that high-field Mössbauer data might provide insight into other possible low-symmetry cases in heme proteins: likely candidates are the T-state forms of deoxyhemoglobin. A tilt of the proximal histidine has been observed in deoxyhemoglobin;[49−51] spectroscopic data have been offered to suggest the functional significance of such tilts in cooperative oxygen binding by hemoglobin.[52]

Thus, the significance of the unusual Mössbauer features of the new crystalline form of [Fe(TPP)(2-MeHIm)] needs to be explored further. The characterization, both by Mössbauer and by structural methods, of additional five-coordinate imidazole-ligated iron(II) porphyrinates is needed. Other studies into the electronic structure of [Fe(TPP)(2-MeHIm)] and related species would also be informative. Single-crystal Mössbauer studies and evaluation of the zero-field splitting constant (D) from temperature-dependent magnetic susceptibility measurements are significant candidates. In view of the difficulties of interpreting the data of the various five-coordinate imidazole-ligated iron(II) porphyrinates, it remains true that, as noted by Debrunner in his important review,[36] "...the electronic state of iron in ferrous porphyrins, important as it is biologically, is still incompletely understood."

Synthetic and Structural Studies. The preparation of high-spin, five-coordinate iron(III) or iron(II) porphyrin species with neutral axial ligands is difficult. As noted in the Introduction, the difficulty arises from the large driving force for the binding of a second axial ligand to give six-coordinate species. The equilibrium constant for binding of the second ligand (K_2) is 10 or more times larger than K_1

(46) While the large number of parameters implies that there is not a unique fit to our data, we were unable to to find an acceptable fit without rotating the electric field gradient.

(47) Champion, P. M.; Lipscomb, J. D.; Münck, E.; Debrunner, P. G.; Gunsalus, I. C. *Biochemistry* **1975**, *14*, 4151.
(48) Champion, P. M.; Chiang, R.; Münck, E.; Debrunner, P. G.; Hager, L. P. *Biochemistry* **1975**, *14*, 4159.
(49) Baldwin, J. M.; Chothea, C. *J. Mol. Biol.* **1979**, *129*, 175.
(50) Pulsinelli, P. D. *J. Mol. Biol.* **1973**, *74*, 57.
(51) Heidner, E. J.; Ladner, R. C.; Perutz, M. F. *J. Mol. Biol.* **1976**, *104*, 707.
(52) Friedman, J. M.; Scott, T. W.; Stepnoski, R. A.; Ikeda-Saito, M.; Yonetani, T. *J. Biol. Chem.* **1983**, *258*, 10564.

for typical nitrogenous bases.[53,54] Special strategies are therefore required to prepare five-coordinate imidazole-ligated iron(II) porphyrinate species.

One such strategy for iron(II) species, originally reported by Collman and Reed,[6] involves using a sterically hindered ligand that will reduce the binding constant for the second axial ligand while apparently not significantly affecting K_1. Their preparation of a five-coordinate high-spin iron(II) species made use of the sterically hindered 2-methylimidazole ligand. The 2-methyl group adjacent to the coordinated nitrogen atom creates a steric interaction with the porphyrin core. But, because this species is high spin with the iron atom displaced out of the porphyrin core toward the axial ligand, steric interactions are expected to be minimal. The binding of a second axial ligand, however, would lead to a low-spin species with the iron in the plane, and severe steric interactions between both ligands and the porphyrin core would result. This is, in fact, observed in the six-coordinate complex $[Fe(TPP)(2\text{-}MeHIm)_2]^+$ [34] and the related iron(III) species, $[Fe(TMP)(1,2\text{-}Me_2Im)_2]^+$.[35] Although the use of 2-methylimidazole allows the isolation of a five-coordinate species by significantly reducing K_2, there is concern that the imposed steric effects from the 2-methyl group could influence the coordination parameters at iron. Indeed, a comparison of the coordination group geometry of the five-coordinate [Co(TPP)(1-MeIm)][55] and $[Co(TPP)(1,2\text{-}Me_2\text{-}Im)]$[56] derivatives is consistent with the bulky methyl group leading to both an increased displacement of the cobalt atom and an increased axial $Co-N_{Im}$ bond length in the second complex. The magnitude of the total increase amounts to 0.10 Å. The effects of the sterically bulky methyl group of an imidazole are expected to be more pronounced in the cobalt(II) systems than in the iron(II) systems owing to the substantially smaller out-of-plane displacement of cobalt-(II).

A second strategy for five-coordinate derivatives employs facially hindered porphyrins. These porphyrins limit the access to one face and hence limit the access of a second ligand. A successful design required both the presence of straps and pickets on one side of the porphyrin plane. Sterically unhindered ligands can then be used to study the stereochemical features of high-spin five-coordinate species. There is still concern with this method, however, because of the presence of the straps and pickets that may influence the porphyrin core conformation. In addition, adding large peripheral groups to the porphyrin ligand will invariably reduce the quality of the crystallographic data.

Five-coordinate imidazole-ligated iron(II) species utilizing both of these strategies have been structurally characterized.[8,10,27] Selected geometrical values from these three structure determinations are given as the first three entries in Table 2 and provide reference points for considering the present molecular structure of [Fe(TPP)(2-MeHIm)]. A comparison of the differences observed for these three imidazole systems suggested that the 2-methyl imidazole substituent could affect the out-of-plane iron atom displacement, the degree of tilting of the $Fe-N_{Im}$ bond from the normal to the porphyrin plane, and the degree of tipping of the imidazole from the $Fe-N_{Im}$ vector. The present structure determination of [Fe(TPP)(2-MeHIm)] shows that, while these effects may be present, other effects from the coordination group asymmetry that results from the hindered imidazole are also possible.

The overall structural features of the [Fe(TPP)(2-MeHIm)] molecule are those expected for a high-spin iron(II) complex.[57] These include an expanded porphinato core, large equatorial $Fe-N_p$ bond distances, and a significant out-of-plane displacement of the iron(II) atom. Although these structural features are a result of the large size of the high-spin iron(II) ion, an examination of these iron(II) values in Table 2 shows that there is significant variation within the set of high-spin five-coordinate iron(II) derivatives. The value of the average $Fe-N_p$ bond distance varies from 2.072 up to 2.114 Å. The averaged value observed for [Fe(TPP)(2-MeHIm)] is seen to be at the lower end of the range, but there is an interesting pattern in the $Fe-N_p$ distances that will be discussed subsequently. The out-of-plane displacements of the iron atom out of the mean 24-atom porphyrin core and the plane defined by the four pyrrole nitrogen atoms also display a large range of values. The displacement ranges are 0.34−0.65 Å out of the 24-atom plane and 0.31−0.56 Å out of the four pyrrole nitrogen atom plane. The out-of-plane displacements for the two [Fe(TPP)(2-MeHIm)] derivatives are seen to be different; this suggests that the presence of a hindered imidazole ligand does not necessarily lead to larger values of displacements. Indeed, the 1-methylimidazole derivative given in Table 2 ($[Fe(Piv_2C_8P)(1\text{-}MeIm)]$[27]) has the same value of ΔN_4.[58]

The large iron(II) ion is accommodated in the central hole of the porphyrin ring not only by the large iron atom displacements and long $Fe-N_p$ bond distances but also by a radial expansion of the core (an increase in the size of the central hole).[63] Again, as seen in Table 2, there is significant variation in the values for the radius of the central hole, which range from 2.030 to 2.051 Å for the five-coordinate high-

(53) Nesset, M. J. M.; Shokhirev, N. V.; Enemark, P. D.; Jacobson, S. E.; Walker, F. A. *Inorg. Chem.* **1996**, *35*, 5188.
(54) Safo, M. K.; Nesset, M. J. M.; Walker, F. A.; Debrunner, P. G.; Scheidt, W. R. *J. Am. Chem. Soc.* **1997**, *119*, 9438.
(55) Scheidt, W. R. *J. Am. Chem. Soc.* **1974**, *96*, 90.
(56) Dwyer, P. N.; Madura, P.; Scheidt, W. R. *J. Am. Chem. Soc.* **1974**, *96*, 4815.
(57) Scheidt, W. R.; Reed, C. A. *Chem. Rev.* **1981**, *81*, 543.
(58) A reviewer has raised the question of the effect of the axial ligand basicity on the structural parameters, especially those of the iron displacement and axial ligand to iron bond distance and tilt. There are inadequate data to recognize any possible trend or not. However, ligand basicity would appear to play a minor role, at most, in any variation in axial ligand interactions based on the behavior of six-coordinate iron(II)[54,59] and iron(III).[60−62]
(59) Safo, M. K.; Scheidt, W. R.; Gupta, G. P. *Inorg. Chem.* **1990**, *29*, 626.
(60) Safo, M. K.; Gupta, G. P.; Walker, F. A.; Scheidt, W. R. *J. Am. Chem. Soc.* **1991**, *113*, 5497.
(61) Safo, M. K.; Gupta, G. P.; Watson, C. T.; Simonis, U.; Walker, F. A.; Scheidt, W. R. *J. Am. Chem. Soc.* **1992**, *114*, 7066.
(62) Safo, M. K.; Walker, F. A.; Raitsimring, A. M.; Walters, W. P.; Dolata, D. P.; Debrunner, P. G.; Scheidt, W. R. *J. Am. Chem. Soc.* **1994**, *116*, 7760.
(63) Scheidt, W. R.; Gouterman, M. In *Iron Porphyrins, Part One*; Lever, A. B. P., Gray, H. B., Eds.; Addison-Wesley: Reading, MA, 1983; p 89.

spin iron(II) species. The largest values for the central radius are only slightly smaller than the 2.057 Å value found for six-coordinate, high-spin [Fe(TPP)(THF)$_2$] where the iron is presumably constrained by the two equivalent axial interactions to be centered in the porphyrin plane.[13]

The iron atom displacement from the 24-atom mean plane (Δ, Table 2) and the four nitrogen atom plane (ΔN_4) are seen to be different and sometimes significantly different for any given derivative. The difference in the two values (note that Δ is always larger than ΔN_4) is a measure of porphyrin core doming. Porphyrin core doming is observed for metalloporphyrin derivatives with metal ions that are too large to fit into the central hole of the porphyrin ring.[64] The size of the iron(II) ion would appear to be at the lower edge of metal ion size leading to core doming; much less doming is observed for five-coordinate high-spin iron(III) derivatives where the high-spin iron(III) ion is slightly smaller.

The range of values observed for the geometric variables responsive to the metal ion size reflects the subtle interplay of the attractive and repulsive interactions between iron, the porphyrin ligand, and the axial ligand. No single stereochemical feature is so dominated by the large size of the high-spin iron(II) that a near constant value is observed. This variability is much larger than that of, for example, high-spin iron(III) porphyrinates. Additionally, however, there are stereochemical features for [Fe(TPP)(2-MeHIm)] specific to the presence of the sterically hindered imidazole ligand.

Possible, and previously recognized, specific stereochemical features that can accommodate the bulky 2-methyl group of imidazole include a lengthening of the axial Fe$-$N$_{Im}$ bond length, off-axis tilting of the Fe$-$N$_{Im}$ bond, rotation of the imidazole leading to unequal Fe$-$N$_{Im}-$C$_{Im}$ angles, and the relative orientation of imidazole plane with respect to the porphyrin core. The structure of [Fe(TPP)(2-MeHIm)] now also reveals that the bulky methyl group can lead to porphyrin core conformational features and an accompanying asymmetry in the equatorial Fe$-$N$_p$ bonds. We consider the previously recognized features first. Finally, we will note a stereochemical feature we believe is caused by the 2-methyl substituent that has not been previously recognized.

The Fe$-$N$_{Im}$ bond length to the major orientation of the imidazole ligand in [Fe(TPP)(2-MeHIm)] is 2.127(3) Å, which is similar to that observed in [Fe(Piv$_2$C$_8$P)(1-MeIm)] but shorter that than observed in [Fe(TPP)(2-MeHIm)](2-fold). Thus, the presence of the 2-methyl group does not necessarily lead to a longer axial Fe$-$N$_{Im}$ bond length. Differences in the axial lengths in the two forms of [Fe(TPP)(2-MeHIm)] are consistent with differences in the orientation of the axial ligand plane with respect to the directions defined by the Fe$-$N$_p$ bonds. In [Fe(TPP)(2-MeHIm)](2-fold), the dihedral angle between the imidazole plane and the closest Fe$-$N$_p$ vector (ϕ) is 6.5°, a value typical for coordinated imidazoles, which tend to be quite small.[65] The ϕ value of 24.0° in [Fe(TPP)(2-MeHIm)] is consistent with the shorter axial bond length.

The steric bulk of the 2-methyl group leads to, in all derivatives examined to date and for all metal species and spin states, an off-axis tilt of the axial M$-$N$_p$ bond and a rotation of the imidazole ligand that leads to unequal Fe$-$N$_{Im}-$C$_{Im}$ angles. Values for these variables for [Fe(TPP)(2-MeHIm)] and other iron(II) and iron(III) imidazole species are given in Table 2. The off-axis tilt and imidazole rotation are correlated so as to maximize the distance between the 2-methyl group and porphyrin core atoms. This is clearly visible in Figure 1. The distance of the closest hydrogen of the methyl group of the major imidazole to a nitrogen of the porphyrin core is 2.78 Å (N(1)···H(4b)). The hydrogen bound to C(2) now becomes closer to the porphyrin plane because of the tilt and ligand rotation. The H(2)···N(3) distance is 2.79 Å.

Interestingly, there are two low-spin six-coordinate hindered imidazole derivatives of iron(III). Both species have imidazoles with large ϕ angles and relative perpendicular orientations of the two axial ligands to alleviate the steric interactions of the 2-methyl substituent with the porphyrin core. The off-axis tilts are less than in the five-coordinate species; the iron is in the porphyrin core plane, which is then severely ruffled to accommodate the 2-methyl groups. The porphyrin core conformation in [Fe(TPP)(2-MeHIm)] has unusual features that merit further comment. In addition to the modest porphyrin core doming already noted (0.06 Å), the porphyrin core also has a substantially stepped or wave conformation component. This type of conformation and especially the magnitude of the components are relatively unusual for an iron derivative. Indeed, to our knowledge, such a conformation has not been observed in a five-coordinate iron(II) porphyrinate. The conformational components are most readily seen from the perspective of atomic displacements from the mean plane of the four pyrrole nitrogen atoms (Figure 2). Two adjacent pyrrole rings are tilted down (away) from this mean plane, while the other two (opposite) pyrrole rings are tilted slightly above the plane of the four nitrogen atoms as can be clearly seen in Figure 1. This appears to result from an accommodation of the bulky methyl group. The imidazole has both tilted and rotated to minimize the 2-methyl···porphyrin core interactions, but additionally, the porphyrin core has also adjusted to minimize the contacts. The arrangement of the methyl hydrogen atoms and the entire imidazole ligand with respect to the porphyrin core can be seen in Figure 4. The effect of the 8.3° off-axis tilt of the imidazole can also be visualized in Figure 4 where the proton-substituted nitrogen atom is seen to be almost directly above the iron atom. Unfortunately, it is impossible to determine if such conformational effects are present in the structures of [Fe(TPP)(2-MeHIm)](2-fold)[8] and [Fe(TpivPP)(2-MeHIm)].[10] Both have crystallographically demanded 2-fold symmetry, which leads to disorder of the axial ligand and also limits any possibility of identifying subtle core conformational effects from the interaction of the axial ligand due to the "averaging" of the porphyrin ligand over two positions 180° from each other. However, in the five-coordinate cobalt derivative [Co(TPP)(1,2-Me$_2$Im)], there is an asymmetry in the saddled core conformation that can be

(64) Scheidt, W. R.; Lee, Y. J. *Struct. Bonding (Berlin)* **1987**, *64*, 1.
(65) Scheidt, W. R.; Chipman, D. M. *J. Am. Chem. Soc.* **1986**, *108*, 1163.

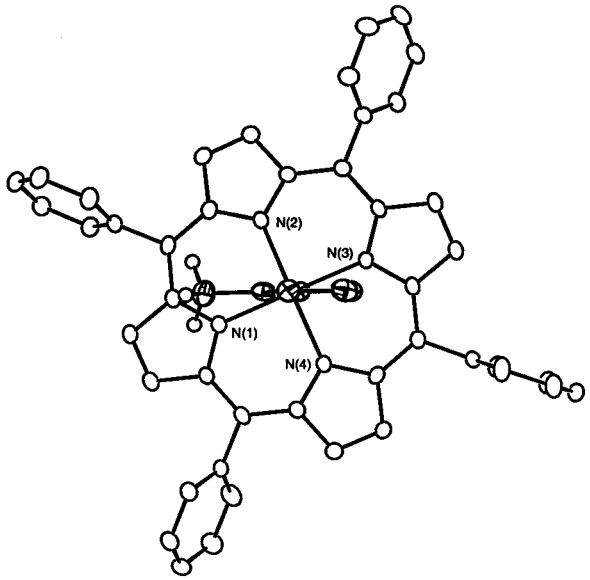

Figure 4. ORTEP diagram of [Fe(TPP)(2-MeHIm)] showing the orientation of the 2-methylimidazole ligand with respect to porphyrin core atoms. The four nitrogen atom mean plane is parallel to the plane of the paper.

attributed to the steric effects of the 2-methyl group. In [Co(TPP)(1,2-Me_2Im)], the one pyrrole ring that has significantly larger displacements is associated with the position of the imidazole and the methyl group. Of course, the degree of steric stress of the 2-methyl group of coordinated imidazole depends on a number of factors including orientation of the axial imidazole, the magnitude of the iron out-of-plane position, and the magnitude of core doming.

A final and unexpected stereochemical feature is an apparent correlation of axial ligand tilting and core conformation with an asymmetry in the equatorial bond distances. There are two short Fe−N_p bond lengths (average 2.066(4) Å) and two long bond lengths (average 2.081(3) Å, confer Figure 2); the difference is statistically significant. The combination of the off-axis tilt and core conformation apparently leads to a stronger interaction of iron with two pyrrole nitrogen atoms. Similar nonplanarity and nonequivalent Fe−N_p bonds could also be present in the previously characterized species with imidazole ligands but are obscured by the crystallographically required 2-fold symmetry. Such asymmetric bonding interactions could also arise in response to off-axis tilts of the proximal histidine in heme proteins. Histidine tilts have been observed in protein structure determinations and have been especially noted in a number of hemoglobin derivatives, but any equatorial asymmetry is unlikely to be be discernible in protein structures.

It is interesting to speculate, but at the moment, it remains speculation, that some or all of the distortions around the iron that may be different in the two forms of [Fe(TPP)(2-MeHIm)] lead to the broadened Mössbauer spectrum in the present case but not for [Fe(TPP)(2-MeHIm)](2-fold). If that is true, then the similarly broadened Mössbauer spectra also observed in deoxymyoglobin and deoxyhemoglobin imply that [Fe(TPP)(2-MeHIm)] is a better structural and electronic model for the five-coordinate oxygen-carrying hemoprotein.

Changes in the coordination group stereochemistry of iron(II) porphyrinates with a sterically hindered axial ligand appear to be subtle, complex, and interrelated. The possible effects of the 2-methyl substituent in the current complex include increase in ϕ angle, distortions of the core, tilting/tipping of the imidazole, and induced asymmetry in the equatorial Fe−N bonds. It is presumed that these interrelated effects have achieved the most favorable geometry. The most surprising feature of the effects seen in the present result is that porphyrin core deformations are apparently preferred relative to axial bond distance elongation as a response to steric stress. The structural and Mössbauer results both show the remarkable pliability of iron(II). It remains a challenge to the structural chemist to define the relative importance of these structural effects and which can have functional significance in heme proteins.

Acknowledgment. We thank the National Institutes of Health for support of this research under Grant GM-38401 to W.R.S. Funds for the purchase of the FAST area detector diffractometer was provided through NIH Grant RR-06709 to the University of Notre Dame.

Supporting Information Available: Tables S1−S6, giving complete crystallographic details, atomic coordinates, anisotropic temperature factors, fixed hydrogen atom positions, and complete listings of bond distances and angles; Figure S1, an ORTEP diagram of [Fe(TPP)(2-MeHIm)] showing the two orientations of the imidazole ligand; Figure S2, a formal diagram giving atomic displacements from the 24-atom man plane; and Figure S3, showing a side-on view of the molecule with the mean plane perpendicular to the plane of the paper. This material is available free of charge via the Internet at http://pubs.acs.org.

IC020012G